ISSN: 2319-5967
ISO 9001:2008 Certified
International Journal of Engineering Science and Innovative Technology (IJESIT)
Volume 4, Issue 5, September 2015

Effect of dysprosium substitution on structural and magnetic properties of cobalt ferrite nanoparticles

Sheena Xavier[a*], Rintu Mary Sebastian[b] and E. M. Mohammed[b]
[a]Department of Physics, St. Xavier's College for Women, Aluva, Kerala 683101, India
[b]Research Department of Physics, Maharaja's College, Ernakulam, Kerala 682011, India
[*]Corresponding author: Sheena Xavier, Associate Professor, Department of Physics, St. Xavier's College for Women, Aluva.

Abstract: ***Dysprosium substituted cobalt ferrite nanoparticles ($CoFe_{2-x}Dy_xO_4$) have been prepared through the sol-gel technique. X-ray diffraction analysis reveals the formation of cubic spinel structure in all the samples. The average crystallite size was estimated using Hall-Williamson analysis and lies in 16 to 24 nm regime. The lattice parameter increases with dysprosium ion concentration and this suggests the expansion of the unit cell with doping. Minor presence of orthoferrite phase is noticed in samples with higher dysprosium content. The transmission electron micrographs show the spherical shape and narrow size distribution of the nanoparticles. The infrared spectra indicate the substitution of dysprosium ions in octahedral sites. The elemental composition of the prepared samples was checked by X-ray fluorescence analysis. The saturation magnetization and coercivity are found to decrease with increase in dysprosium content and about 90% reduction in magnetic hysteresis loss is observed for $CoFe_{1.75}Dy_{0.25}O_4$.***

Index Terms**- Cobalt ferrite, Dy^{3+} substitution, lattice parameter, particle size, magnetic properties.**

I. INTRODUCTION

Nanocrystalline ferrites are important magnetic materials which have recently attracted a great deal of attention due to wide range of technological and biomedical applications. The diverse applications of magnetic nanoparticles demand the modulation of structural parameters such as size, shape and morphology. Many efforts are taken by researchers in the material science to tailor the properties of the spinel ferrites to satisfy the requirements of specific application. The structural properties of ferrites are highly influenced by the method of preparation, sintering conditions, substitution of various cations and cation distribution [1], [2]. Several chemical and physical methods are available for the synthesis of ferrite nanoparticles. The sol gel technique gained the attention of researchers because of its advantages such as production of nanoparticles with good chemical homogeneity, small size and narrow size distribution [3], [4].

Cobalt ferrite is an important member of the ferrite family and adopts partially inverse spinel structure. The degree of inversion and the distribution of cations on the tetrahedral (A) and octahedral (B) sites of the spinel structure depend on the method of preparation and heat treatment [5], [6]. The remarkable magnetic and electric properties of cobalt ferrite include high coercivity, moderate saturation magnetization and high electrical resistivity. These properties along with good chemical stability and mechanical hardness make it suitable for high density recording media, magnetic fluids, biomedical drug delivery and sensors [7]-[9]. Rare earth ions are promising substitutes for improving the properties of spinel ferrites. Several researchers have investigated the structural and magnetic properties of rare earth doped ferrites [10]-[12]. The substitution of rare earth ions with large ionic radii in spinel ferrites is expected to induce strain and to significantly modify the structural and magnetic properties. Rare earth doped ferrites with modified properties find applications in enhanced magnetic storage, electronic and microwave devices and catalysis [13]-[15]. Recently Bamzai et al. [16] have studied the effect of dysprosium substitution on the structural and magnetic properties of magnesium ferrite. They found that the lattice constant increased with an increase in dysprosium concentration. Kumar et al. [17] have indicated a significant reduction in the dielectric parameters through the doping of La^{3+} in cobalt ferrite synthesized by co-precipitation route. However, a systematic study on the structural and magnetic properties of dysprosium doped cobalt ferrite is rarely reported. Moreover, in almost all reported investigations on rare earth doped ferrites, synthesis technique employed is high temperature solid state reaction and sintering above 1000 K which resulted in the formation of secondary orthorhombic phase [14], [16]. Hence the changes observed in the properties of ferrites may be due to the substitution of rare earth ions in the spinel lattice or attributed to the secondary phase formation. In this paper we report the effect of dysprosium (Dy) substitution on the structural and magnetic properties of cobalt ferrite nanoparticles. The samples synthesized through the low temperature sol gel technique

ISSN: 2319-5967
ISO 9001:2008 Certified
International Journal of Engineering Science and Innovative Technology (IJESIT)
Volume 4, Issue 5, September 2015

and sintered at 773 K exhibits single phase spinel structure for small concentrations of dysprosium. Further, we observed a minor presence of $DyFeO_3$ phase only in compositions with higher dysprosium content. Therefore the modifications observed in the properties of the cobalt ferrite samples can be attributed to the substitution of dysprosium in spinel lattice. Our present work aims to study the effect of Dy^{3+} substitution on the structural and magnetic properties of sol – gel synthesized nanocrystalline cobalt ferrite.

II. EXPERIMENT

A. Synthesis

Dysprosium substituted cobalt ferrite nanoparticles $CoFe_{2-x}Dy_xO_4$ (x=0.0 to 0.25 in steps of 0.05) were synthesized by the sol-gel technique. Stoichiometric ratios of analytical reagent grade cobalt nitrate (Co $(NO_3)_2.6H_2O$), dysprosium nitrate (Dy $(NO_3)_3.xH_2O$) and ferric nitrate (Fe $(NO_3)_3.6H_2O$) were used. The details of the synthesis technique are already reported in our previous work [2]. The obtained powder was ground well and sintered for 4 hours in a muffle furnace at 773 K. Cylindrical disc shaped pellets of the samples (13mm diameter and 2-3 mm thickness) were made using a pelletizer by applying a pressure of 8 tons. These pellets were sintered in air at 773 K for 10 hours and were subsequently cooled.

B. Characterization

The structural characterization of the prepared samples were done using X-ray powder diffractometer (Bruker AXS D8 Advance) with Cu-Kα radiation (λ = 1.5406 Å) at 40 kV and 35 mA. The shape, size and size distribution of the nanoparticles were analyzed by using transmission electron microscope (Philips-CM200). The selected area electron diffraction patterns of the samples were also recorded. The Fourier transform infrared spectrometer (Thermo Nicolet, Avatar 370) was used to record the absorption spectra of the samples. The elemental composition of the samples was examined using wavelength dispersive X-ray fluorescence spectrometer (Bruker S4-Pioneer). The Magnetic characterization was carried out using a vibrating sample magnetometer (Lakeshore 7410) at room temperature.

III. RESULT AND DISCUSSION

A. Structural analysis

X-ray diffraction (XRD) pattern of $CoFe_{2-x}Dy_xO_4$ (x=0.0 to 0.25 in steps of 0.05) is shown in Fig.1. The diffraction peaks corresponding to the planes (220), (311), (222), (400), (422), (511) and (440) are observed in all the samples. The patterns were compared with standard data for cobalt ferrite (JCPDS PDF Card No. 22-1086) and it can be concluded that all the samples exhibit a cubic spinel structure. Small peaks corresponding to secondary phase are observed for samples with higher dysprosium content. Rare earth doped systems may have secondary phases in addition to the pure spinel phase. Bharathi et al. [18] indicated the presence of $DyFeO_3$ phase in Dy doped nickel ferrite system. Peng et al. [9] have reported formation of secondary phase in cobalt ferrite when it is doped with 15% of gadolinium ions. However, in the present study, growth of secondary orthoferrite phase is observed from x=0.2 onwards and the low intensity of the secondary peak implies that the major part of Dy^{3+}ions are occupying the octahedral sites of the spinel lattice and only small amount of dysprosium form the $DyFeO_3$ phase. The large ionic radii of the dysprosium ions make it difficult to enter the spinel lattice and that can put a limit on the amount of rare earth doping in ferrites.

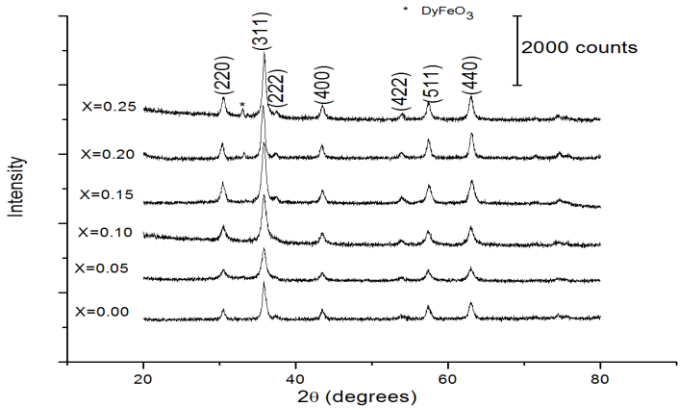

Fig. 1: XRD pattern of $CoFe_{2-x}Dy_xO_4$ system

ISSN: 2319-5967
ISO 9001:2008 Certified
International Journal of Engineering Science and Innovative Technology (IJESIT)
Volume 4, Issue 5, September 2015

The interplanar spacing d_{hkl} is calculated using Bragg's equation which in turn is used to estimate the lattice parameter '*a*' for the prominent diffraction peak (311) using the following equation [19].

$$a = d_{hkl}\sqrt{h^2 + k^2 + l^2} \qquad (1)$$

The average crystallite size of the samples is estimated from Hall – Williamson plots [20], [21]. We have observed that dysprosium doping has induced positive strain in all the investigated samples. Fig. 2 depicts these plots for the sample with x=0.0. The actual (X-ray) density of the samples was calculated using the formula [23]

$$\rho_x = \frac{8M}{Na^3}, \qquad (2)$$

where *M* is the molecular weight (Kg) of the sample, *N* is Avogadro's number (per mol) and *a* is the lattice parameter (Å). Bulk densities of the samples were determined using the formula

$$\rho_b = \frac{m}{\pi r^2 h}, \qquad (3)$$

where *m* is the mass (Kg), *r* is the radius (m) and *h* is the height of the pellet (m). Percentage of porosity was calculated using the following formula [24]

$$P = \left(1 - \frac{\rho_b}{\rho_x}\right)100 \qquad (4)$$

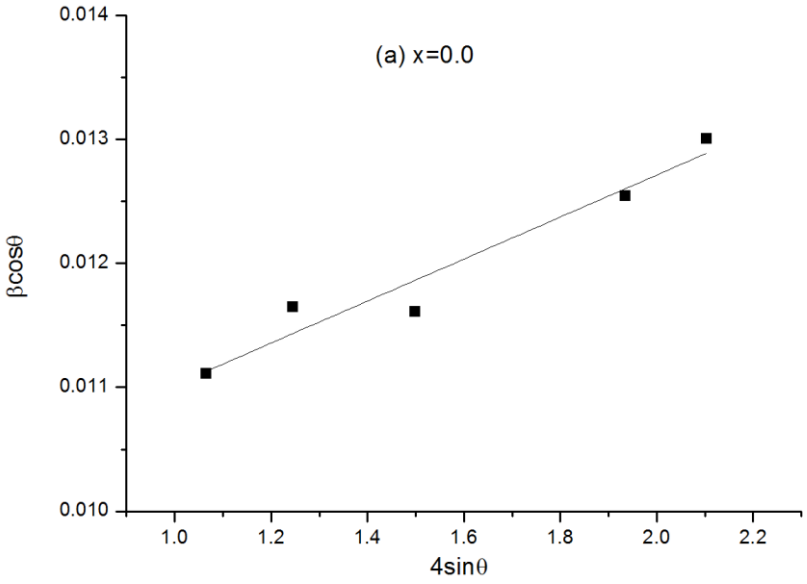

Fig 2: Hall – Williamson plots of $CoFe_2O_4$

The crystallite size of the samples is observed to increase with dysprosium concentration. This is consistent with the results reported for Gd^{3+}doped cobalt ferrite [9], Nd^{3+} doped zinc ferrite [15] and Dy^{3+} doped Ni-Co ferrite [25]. The observed increase in the lattice parameter of cobalt ferrite with Dy substitution may be attributed to the replacement of smaller Fe^{3+} ions (0.0645nm) at the octahedral site by larger Dy^{3+} ions (0.0912nm). This causes an expansion of unit cell and it is in agreement with the existing literature [26, 27]. A slight decrease in the lattice parameter is noticed when the dysprosium content exceeds x=0.2. This may be an indication of the solubility limit of Dy ions in the spinel lattice. Beyond this limit, the redundant dysprosium ions cannot enter the spinel lattice and leads to the formation of the $DyFeO_3$ phase on the grain boundaries. The rate of increase in the crystallite size also shows a decline for samples with high dysprosium content. Similar behaviour has been reported by Jing et al. [28] in Gd doped lithium nickel ferrite system and explained in terms of the compression of the spinel lattice induced by secondary phase. Thus, for compositions with higher dysprosium content, the

ISSN: 2319-5967
ISO 9001:2008 Certified
International Journal of Engineering Science and Innovative Technology (IJESIT)
Volume 4, Issue 5, September 2015

secondary phase formation hinders the expansion of the lattice with the result that further grain growth is inhibited. The lattice parameter (*a*) and crystallite size (*D*) obtained for all the samples are given in Table 1.

Table 1: Effect of Dy^{3+} doping on the lattice parameter, crystallite size, density, porosity and particle size of $CoFe_{2-x}Dy_xO_4$ system

Dy Content x	Lattice parameter (Å)	Crystallite size (nm)	X-ray density (gcm^{-3})	Bulk density (gcm^{-3})	Porosity (%)	Particle size (nm)
0.00	8.341	16.55±1.6	5.371	3.862	28.08	20±3
0.05	8.345	18.62±1.7	5.486	3.717	32.24	
0.10	8.350	20.04±1.6	5.598	3.690	34.08	27±3
0.15	8.353	22.70±1.2	5.713	3.581	37.31	
0.20	8.358	23.63±1.8	5.824	3.561	38.84	31±3
0.25	8.354	23.80±1.2	5.948	3.566	40.05	

The study of the density and porosity becomes important for probing into the properties of the prepared samples. The porosity depends on several parameters such as preparation method, grain size, sintering temperature and density. The X-ray density (ρ_x), bulk density (ρ_b) and percentage porosity (*P*) of the studied samples are tabulated in Table 1. The X-ray density increases linearly with dysprosium ion content and this can be correlated with the increase of atomic weight of Dy^{3+} substituted for Fe^{3+} of lower atomic mass. The magnitudes of bulk densities are smaller than that of the corresponding X-ray densities and this difference in magnitude may be attributed to the existence of pores in the bulk samples. The porosity is observed to increase with Dy content. The increase in X-ray density with doping plays a significant role in deciding the porosity of the samples.

B. Transmission electron microscopy

Transmission electron microscope (TEM) images of $CoFe_{1.9}Dy_{0.1}O_4$ sample is shown in Fig. 3. Most of the nanoparticles are almost spherical in shape; however, a slight agglomeration is noticed.

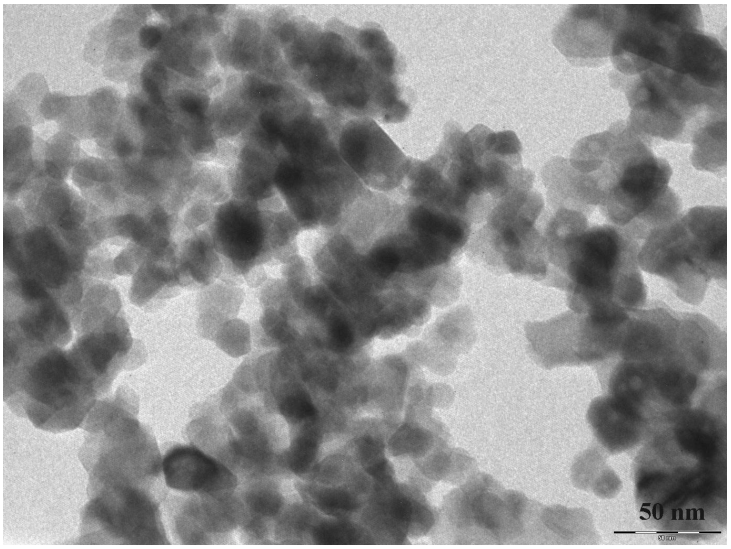

Fig 3: TEM image of $CoFe_{1.9}Dy_{0.1}O_4$

The size of more than 200 nanoparticles is determined from different images of the same sample using *Image J* software and size distribution histograms are drawn. The particle size distribution of the nanoparticles as observed in TEM images is shown in Fig. 4. It can be seen that the samples have narrow size distribution. The most probable diameter of the nanoparticles was determined by modelling the data with log normal distribution. The particle sizes determined from TEM analysis are shown in Table 1.

ISSN: 2319-5967
ISO 9001:2008 Certified
International Journal of Engineering Science and Innovative Technology (IJESIT)
Volume 4, Issue 5, September 2015

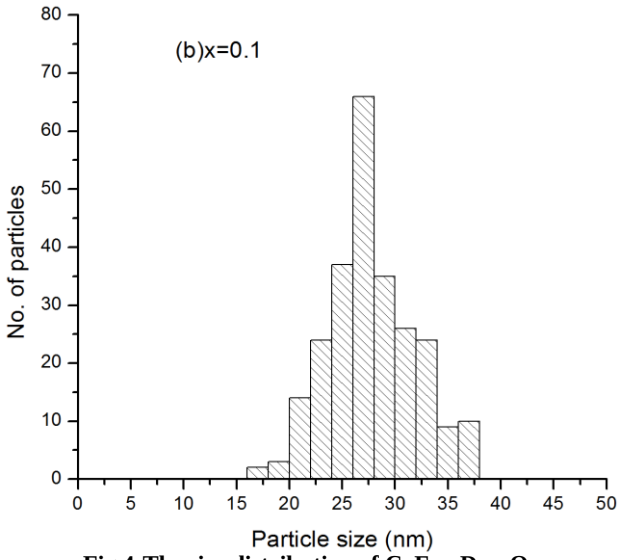

Fig 4:The size distribution of $CoFe_{1.9}Dy_{0.1}O_4$

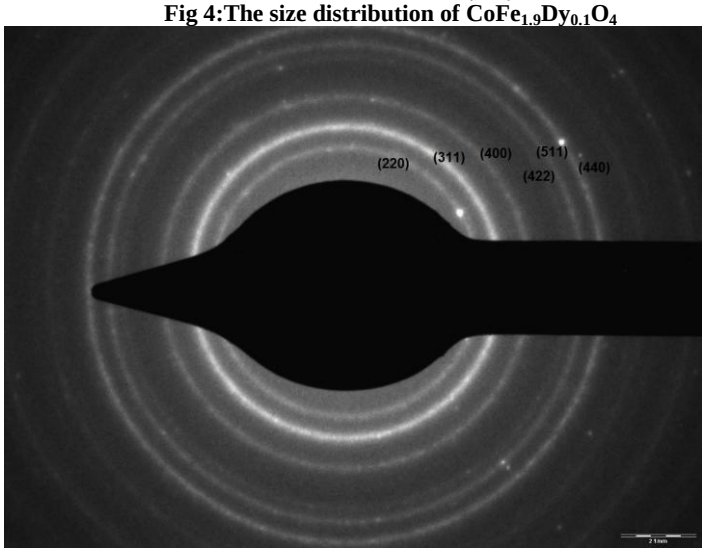

Fig 5: SAED pattern of $CoFe_{1.9}Dy_{0.1}O_4$

The selected area electron diffraction (SAED) pattern of the typical sample is depicted in Fig. 5. The continuous and diffused rings observed in the micrograph indicate the polycrystalline nature of these materials. Every diffraction ring corresponds to a group of lattice planes with the same miller index. The prominent rings observed below the diffraction angle (2θ) of 70^o are marked with their respective *hkl* planes. The emergence of spots in the patterns with higher doping concentration can be attributed to the increase in the average size of the nanoparticles.

C. Infrared spectra analysis

In the wave number range 1000-300 cm^{-1}, the infra red bands of solids are usually assigned to vibration of ions in the crystal lattice. Two prominent metal-oxygen bands are seen in the IR spectra of all spinel ferrites. According to Waldron [29] the vibrations of unit cell of cubic spinel can be constructed in the tetrahedral site (A) and octahedral site (B). The formation of spinel structure in the prepared samples can be confirmed by the presence of characteristic absorption bands in the Fourier transform infrared (FTIR) spectrum. FTIR spectra of the $CoFe_{2-x}Dy_xO_4$ samples in the wave number range 900-400 cm^{-1} are shown in Fig. 6 and the vibrational frequencies of the IR bands are given in Table 3. The absorption bands observed in the range 600-550 cm^{-1} and 450-400 cm^{-1} are characteristic of the spinel ferrites. The higher frequency band (ν_1) corresponds to intrinsic stretching vibrations of the metal at the tetrahedral site and the lower frequency band (ν_2) is caused by the metal – oxygen vibration in the octahedral site [30].

ISSN: 2319-5967
ISO 9001:2008 Certified
International Journal of Engineering Science and Innovative Technology (IJESIT)
Volume 4, Issue 5, September 2015

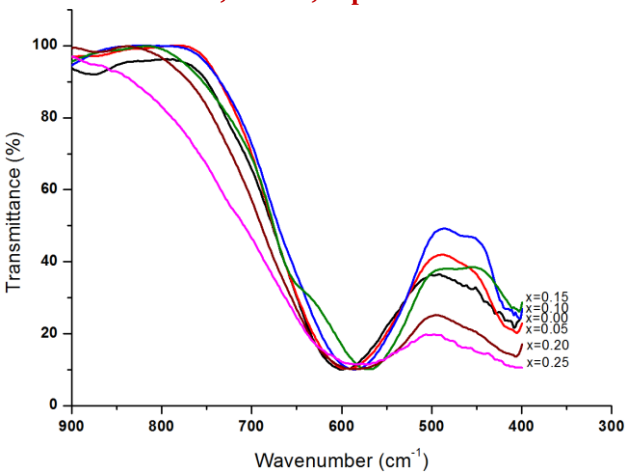

Fig 6: FTIR spectra of $CoFe_{2-x}Dy_xO_4$ system

D. Magnetic properties

Magnetic characterization of the samples was carried out by vibrating sample magnetometer at room temperature with a maximum applied field of 15 kOe.

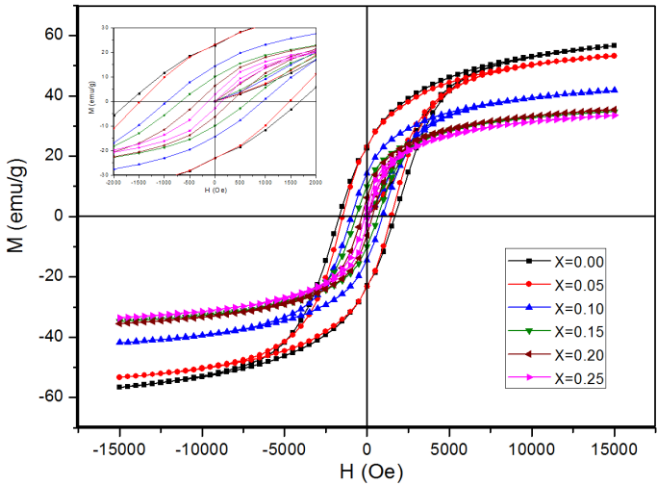

Fig 7: Room temperature hysteresis curves of $CoFe_{2-x}Dy_xO_4$ samples

Fig. 7 shows the typical magnetic hysteresis loops of $CoFe_{2-x}Dy_xO_4$ system and the inset of the figure shows a magnified region around the origin. As can be seen, the saturation magnetization is not achieved in the maximum applied field. This may be due to the non-collinearity of spins on the surface of nanoparticles which makes the alignment of spins difficult even at high applied fields [31]. The saturation magnetization (M_s), coercivity (H_c) and remanent ratio ($R=M_r/M_s$) of all the samples are presented in Table 2. The value of M_s obtained for pure cobalt ferrite is 58.3emu/g. With increase in Dy content saturation magnetization decreases and about 40% reduction is observed for 12.5% doping (x=0.25). The decrease of M_s with Dy content is consistent with the results reported for rare earth doped ferrites [2], [12]. The saturation magnetization of ferrite material depends on the preparation conditions, grain size and cation distribution between the tetrahedral (A) and octahedral (B) sites. The change in the concentration and nature of ions in A and B sites can also affect the saturation magnetization. The decrease in M_s with dysprosium content may be attributed to the weakening of A-B interactions. Three types of interactions are possible between the unpaired electrons of the ions occupying the A and B sites. But the A-B interaction predominates over the A-A and B-B interactions. The net magnetic moment in a ferrimagnetic material is the difference between the moments of B and A sublattice. Due to large ionic radii, Dy^{3+} ions are substituted on the octahedral site of the spinel lattice. Thus the substitution of Fe^{3+} ions by Dy^{3+} ions decreases Fe^{3+}-Fe^{3+} interactions and reduces the magnetic moment of octahedral sublattice, causing

ISSN: 2319-5967
ISO 9001:2008 Certified
International Journal of Engineering Science and Innovative Technology (IJESIT)
Volume 4, Issue 5, September 2015

M_s to decrease. Furthermore, the magnetic moments of rare earth ions are mainly due to the 4*f* electrons and the ordering of their moments occurs at very low temperatures [32]. Hence the effect of Dy^{3+} ions in the cobalt ferrite material seems to be similar to the substitution of non-magnetic atoms in the octahedral Fe sites of the spinel lattices and they contribute very little to the magnetization of the doped cobalt ferrite.

Table 2: Effect of Dy^{3+} doping on magnetic parameters and vibrational frequency band positions of $CoFe_{2-x}Dy_xO_4$ system

Dy Content x	M_s (emu/g)	M_r (emu/g)	H_c (Oe)	R	ν_1 (cm^{-1})	ν_2 (cm^{-1})
0.00	58.3	25.7	1683	0.44	597	410
0.05	54.8	23.1	1478	0.42	595	407
0.10	42.9	14.4	944	0.33	590	405
0.15	35.7	10.0	671	0.27	592	405
0.20	36.5	6.3	324	0.17	-	402
0.25	34.6	2.9	136	0.08	-	-

The inset of Fig. 7 shows a magnified region of hysteresis loops around the origin. It is evident from the figure that the coercivity H_c of dysprosium substituted cobalt ferrite samples decreases monotonically and it varies from 1683 to 136 Oe. Significant reduction in coercivity and remanence is noticed in doped samples with concentration $x \geq 0.2$ and this is in accordance with our earlier report [4]. The decrease in coercivity revealed in our study may be due to the increase in crystallite size of the samples with Dy substitution. It is well established in the literature that in the multi domain region, the coercivity of nano – magnetic particles shows an inverse dependence on particle size [33], [34]. Our result is in agreement with the above mentioned relation. The remanent magnetization also decreases in the same manner as that of the coercive field [35]. The remanent ratio is a characteristic parameter of the magnetic material and it is the ease with the magnetization direction reorients to the nearest easy axis after the removal of the field. It decreases from 0.44 to 0.08 with doping and this can be related to the decrease in anisotropy of the crystal lattice by Dy substitution [36]. The considerable reduction observed in the magnetic hysteresis loss of cobalt ferrite nanoparticles with doping (about 90% reduction for 12.5% doping) can be attributed to grain growth and reduced magneto-crystalline anisotropy. Thus the above results suggest that we can tune the magnetic properties of cobalt ferrite nanoparticles by the selection of appropriate amount of dysprosium ions.

IV. CONCLUSION

In summary, we have studied the effect of dysprosium substitution in $CoFe_{2-x}Dy_xO_4$ with x=0.0, 0.05, 0.1, 0.15, 0.2, 0.25 synthesized by sol-gel technique. XRD analysis has revealed that increase in Dy content increases the crystallite size of the samples. The lattice parameter is found to increase with Dy^{3+} addition, suggesting the expansion of the unit cell. The prepared samples exhibit single phase spinel structure for dysprosium concentration below 10% and a minor presence of $DyFeO_3$ is detected when it exceeds that limit. The nanoparticles have spherical morphology and narrow size distribution. The FTIR spectra indicate the occupancy of Dy^{3+} ions on octahedral sites. Though saturation magnetization and coercivity of cobalt ferrite get reduced by dysprosium substitution, the decrease observed in the latter is prominent. The monotonic decrease in coercivity with Dy substitution can be attributed to the particle size dependence of coercivity in multi domain regime. The incorporation of dysprosium ions into the cobalt ferrite decreases saturation magnetization owing to the decrease in A-B interaction. These results suggest that the structural and magnetic properties of cobalt ferrite nanoparticles can be tuned by the substitution of appropriate amount of dysprosium ions and make it suitable for technological applications.

ACKNOWLEDGMENT

SX acknowledges the University Grants Commission of India for providing teacher fellowship. EMM thanks DST and UGC for the financial support. Authors thank SAIF- CUSAT, Kochi; SAIF-IIT, Madras and SAIF-IIT, Mumbai for providing XRD, FTIR, VSM and TEM facilities.

ISSN: 2319-5967
ISO 9001:2008 Certified
International Journal of Engineering Science and Innovative Technology (IJESIT)
Volume 4, Issue 5, September 2015

REFERENCES

[1] Goldman A, Modern Ferrite Technology, New York: Van Nostrand Reinhold; 1990.

[2] Jacob BP, Thankachan S, Xavier S, Mohammed EM. Effect of Tb^{3+} substitution on structural, electrical and magnetic properties of sol–gel synthesized nanocrystalline nickel ferrite. J Alloys compd 2013; 578: 314 – 9.

[3] Jacob BP, Thankachan S, Xavier S, Mohammed EM. Dielectric behaviour and AC conductivity of Tb^{3+} doped $Ni_{0.4}Zn_{0.6}Fe_2O_4$ nanoparticles. J Alloys compd 2012; 54: 29 – 35.

[4] Thankachan S, Jacob BP, Xavier S, Mohammed EM. Effect of samarium substitution on structural and magnetic properties of magnesium ferrite nanoparticles. J Magn Magn Mater 2013; 348: 140 – 5.

[5] Gul IH, Masqood A. Structural, magnetic and electrical properties of cobalt ferrites prepared by the sol – gel route. J Alloys compd 2008; 465: 227 – 31.

[6] Zi Z, Sun Y, Zhu X, Song W. Synthesis and magnetic properties of $CoFe_2O_4$ ferrite nanoparticles. J Magn Magn Mater 2009; 321:1251 – 5.

[7] Gopalan V, Joy PA, Al-Omari IA, Kumar DS,Yoshida Y, Anantharaman MR. On the structural, magnetic and electrical properties of sol – gel derived nanosized cobalt ferrite. J Alloys compd 2009; 485: 711 – 7.

[8] George M, Nair SS, Malini KA, Joy PA, Anantharaman MR. Finite size effects on the electrical properties of sol-gel synthesized $CoFe_2O_4$ powders: Deviation from Maxwell-Wagner theory and evidence of surface polarization effects. J Magn Magn Mater 2006; 302: 190 – 5.

[9] Sanpo N, Christopher CB, Cuie W, James W. Transition metal substituted cobalt ferrite nanoparticles for biomedical applications. Acta Biomater 2013; 9: 5830 – 7.

[10] Jacob BP, Thankachan S, Xavier S, Mohammed EM. Effect of Gd^{3+} doping on the structural and magnetic properties of nanocrystalline Ni-Cd mixed ferrite. Phys Scr 2010; 84: 045702 – 6.

[11] Guo L, Shen X, Meng X, Feng Y. Effect of Sm^{3+} ions doping on structure and magnetic properties of nanocrystalline $NiFe_2O_4$ fibers. J Alloys compd 2010; 490: 301 – 6.

[12] Peng J, Hojamberdiev M, Xu Y, Cao B, Wang J, Wu H. Hydrothermal synthesis and magnetic properties of gadolinium – doped $CoFe_2O_4$ nanoparticles. J Magn Magn Mater 2011; 323: 133 – 8.

[13] Tahar LB, Smiri LS, Artus M, Joudrier AL, Herbst F, Vaulay MJ et al. Characterization and magnetic properties of Sm – and Gd- substituted $CoFe_2O_4$ nanoparticles prepared by forced hydrolysis in polyol. Mat Res Bull 2007; 42: 1888 – 96.

[14] Gadkari AB, Shinde TJ, Vasambekar PN. Structural synthesis of Y^{3+} doped Mg-Cd ferrites prepared by oxalate co-precipitation method. Mater Chem Phys 2009; 114: 505 – 10.

[15] Shinde TJ, Gadkari AB, Vasambekar PN. Effect of Nd^{3+} substitution on structural and electrical properties of nanocrystalline zinc ferrite. J Magn Magn Mater 2010; 322: 2777 – 81.

[16] Bamzai KK, Kour G, Kour B, Kulkarni SD. Effect of cation distribution on structural and magnetic properties of Dy substituted magnesium ferrite. J Magn Magn Mater 2013; 327: 159 – 66.

[17] Kumar P, Sharma SK, Knobel M, Singh M. Effect of La^{3+} doping on the electric, dielectric and magnetic properties of cobalt ferrite processed by co-precipitation technique. J Alloys compd 2010; 508: 115 – 8.

[18] Bharathi KK, Balamurugan K, Santhosh PN, Pattabiraman M, Markadeyulu G. Magneto capacitance in Dy doped Ni ferrite. Phy Rev B 2008; 77: 172401 – 4.

[19] Cullity BD. Elements of X-ray Diffraction. California: Addison – Wesley; 1978.

[20] Williamson GK, Hall WH. X-ray Line Broadening from filed Aluminium and Wolfram. Acta Metall 1953; 1: 22 – 31.

[21] Thankachan S, Jacob BP, Xavier S, Mohammed EM. Effect of neodymium substitution on structural and magnetic properties of magnesium ferrite nanoparticles. Phys Scr 2013; 87: 025701 – 7.

[22] Xavier S, Jacob BP, Thankachan S, Mohammed EM. Effect of samarium substitution on the structural and magnetic properties of nanocrystalline cobalt ferrite. Journal of Nanoscience 2013; http://dx.doi.org/10.1155/2013/524380.

[23] Sutka A, Mezinskis G, Lusis A. Electric and dielectric properties of nanostructured stoichiometric and excess-iron Ni–Zn ferrites. Phys Scr 2013; 87: 025601 – 7.

ISSN: 2319-5967
ISO 9001:2008 Certified
International Journal of Engineering Science and Innovative Technology (IJESIT)
Volume 4, Issue 5, September 2015

[24] Aghav PS, Dhage VN, Mane ML, Shengule DR, Dorik RG, Jadhav KM. Effect of aluminum substitution on the structural and magnetic properties of cobalt ferrite synthesized by sol–gel auto combustion process. Phys B 2011; 406: 4350 – 5.

[25] Kadam AA, Shinde SS, Yadav SP, Patil PS, Rajpure KY. Structural morphological, electrical and magnetic properties of Dy doped Ni – Co substitutional spinel ferrite. J Magn Magn Mater 2013; 329: 59 – 64.

[26] Ahmed MA, Ateia E, Salah LM, Gamal E. Structural and electrical studies on La^{3+} substituted Ni–Zn ferrites Mater Chem Phys 2005; 92: 310 – 21.

[27] Ishaque M, Islam MU, Khan MA, Rahman IZ, Genson A, Hampshire S. Structural, electrical and dielectric properties of yttrium substituted Nickel ferrites. Phys B Condensed Matter 2010; 405: 1532 – 40.

[28] Jing J, Liangchao L, Feng X. Structural analysis and magnetic properties of Gd- doped Li – Ni Ferrites prepared using rheological phase reaction method. J Rare Earth 2007; 25: 79 – 83.

[29] Waldron RD. Infrared spectra of ferrites. Phy Rev 1955; 99: 1727 – 35.

[30] Modi KB, Rangolia MK, Chhantbar MC, Joshi HH. Study of infrared spectroscopy and elastic properties of fine and coarse grained nickel-cadmium ferrites. J Mater Sci 2006; 41: 7308 – 18.

[31] Priyadarshini P, Pradeep A, Rao PS, Chandrasekharan G. Structural, spectroscopic and magnetic study of nanocrystalline Ni-Zn ferrite. Mater Chem Phys 2009; 116: 207 – 13.

[32] Wilkinson MK, Koehler WC, Wollan EO, Cable JW. Neutron diffraction investigation of magnetic ordering in dysprosium. J Appl Phy 1961; 32: 48 – 9.

[33] Maaz K, Mumtaz A, Hasanain SK, Ceylan A. Synthesis and magnetic properties of cobalt ferrite ($CoFe_2O_4$) nanoparticles prepared by wet chemical route. J Magn Magn Mater 2007; 308: 289 – 95.

[34] Chakraverty S, Bandyopadhyay M. Coercivity of magnetic nanoparticles: a stochastic model. J Phys Condens Matter 2007; 19: 216201 – 16.

[35] Gadkari AB, Shinde TJ, Vasambekar PN. Magnetic properties of rare earth ion (Sm^{3+}) added nanocrystalline Mg-Cd ferrites prepared by oxalate co-precipitation method. J Magn Magn Mater 2010; 322: 3823 – 7.

[36] Shirsath SE, Toksha BG, Jadhav KM. Structural and magnetic properties of In^{3+} substituted $NiFe_2O_4$. Mater Chem Phys 2009; 117: 163 – 8.